VOLUME 9 (SPECIAL ISSUE 1) 2023

ISSN 2454 – 3055

Guest Editor: Dr. S. Mohanasundaram
Assistant Guest Editor: Dr. S.S.Syed Abuthahir

INTERNATIONAL JOURNAL OF ZOOLOGICAL INVESTIGATIONS

Forum for Biological and Environmental Sciences

Published by Saran Publications, India

International Journal of Zoological Investigations Vol. 9 (Special Issue 1), 153-159 (2023)

International Journal of Zoological Investigations

Contents available at Journals Home Page: www.ijzi.net

Editor-in-Chief: Prof. Ajai Kumar Srivastav

Published by: Saran Publications, Gorakhpur, India

ISSN: 2454-3055

Synthesis, Characterization and Antimicrobial Studies of Silver Nanoparticles from *Centella asiatica* Leaves Extract

Philip Arockiaraj S. and Kousalya G.N.*

P.G. and Research Department of Chemistry, G.T.N Arts College (Autonomous), Dindigul, Tamil Nadu, India

**Corresponding Author*

Received: 30th January, 2023; **Accepted:** 5th April, 2023; **Published online:** 21st April, 2023

https://doi.org/10.33745/ijzi.2023.v09ispl1.023

Abstract: The current study describes the extraction and subsequent preparation of silver nanoparticles (AgNPs) from *Centella Asiatica* leaves. Experimental methods such as X-ray diffraction, Scanning Electron Microscopy (SEM), Transmission Electron Microscopy (TEM), and Infrared Spectroscopy were used to examine the biosynthesized AgNPs. The produced AgNPs are effective against *Escherichia coli* and *Staphylococcus aureus*. Evidence from this work supports the use of silver nanoparticles as a drug delivery vehicle, proves their anticorrosive properties, and shows their use in antibacterial activity targeting particular illnesses.

Keywords: *Centella asiatica*, AgNPs, Antimicrobial activity, Scanning Electron Microscopy, Transmission Electron Microscopy, Infrared Spectroscopy, *Escherichia coli*, *Staphylococcus aureus*

Citation: Philip Arockiaraj S. and Kousalya G.N.: Synthesis, characterization and antimicrobial studies of silver nanoparticles from *Centella asiatica* leaves extract. Intern. J. Zool. Invest. 9(Special Issue 1): 153-159, 2023.

https://doi.org/10.33745/ijzi.2023.v09ispl1.023

Introduction

Personalized, transportable, cheaper, safer, and easier-to-administer medical and biotech instruments and procedures are all possible because to nanotechnology's revolutionary potential (Buzea *et al.*, 2007; Saini *et al.*, 2010). Researchers have found that materials with very tiny dimensions (such as nanoparticles, thin films, etc.) radically different characteristics than those shown by the same substances when scaled up. Consequently, there is a virtually infinite scope for developing superior tools, frameworks, and materials (Adams and Baughman, 2005). The qualities may be managed by manipulating the structure and composition on the nm scale. The materials and gadgets created by nanotechnologists have the potential to revolutionise our daily lives. Although nanoscale pumps, switches, and motors now exist, the miniature self-replicating devices envisioned by nanotechnology pioneers are still decades away, if they ever materialise at all (Chavali and Nikolova, 2019). But we know they are effective. Semiconducting quantum dots are nanocrystals that potentially improve medical diagnostic

imaging of living organisms. Lighted with UV radiation, they fluoresce in a rainbow of hues that may be utilised to pinpoint and classify various cellular components and biological processes. Crystals like this may improve optical detection by a factor of up to a thousand, making them a useful tool for a wider range of diagnostic procedures in the life sciences. Biological species' DNA is an efficient molecular machine that can replicate on a nanoscale and create complex structures one molecule at a time. The scientific community has used the word "nano" to describe objects one billionth of a metre in size (10^{-9} m). The study of very small objects, such as atoms and molecules, is known as nanoscience. The reduction of size to nanometers gives materials several advantages, including increased strength, lower weight, greater ductility, and other improvements. Exactly how these materials improve is a considerably more nuanced topic. The properties of nanoparticles differed significantly from those of the bulk materials (Nath and Banerjee, 2013; Bhattacharjee and Ahmaruzzaman, 2015), and this difference was mostly due to the nanoparticles' smaller size. Many fields, including materials and manufacturing, nanoelectronics, medicine, healthcare, energy, biotechnology, IT, and national security, stand to benefit from nanotechnology research. The selection of green or ecologically friendly solvents, excellent reducing agents, and safe ingredients for stabilisation are the three most crucial parameters for nanoparticle synthesis. Nanoparticles may be created by a variety of different synthetic processes, including physical, chemical, and biosynthetic methods. Traditional chemical approaches are sometimes prohibitively costly and fraught with danger because of the toxicity and potential harm to the environment posed by the chemicals they use (Karkaj *et al.*, 2012). Producing nanoparticles for use in biomedical applications via the utilisation of plant and microbial biosynthetic pathways is a safe, biocompatible, ecologically friendly, and green option. Substances at the nanoscale are of paramount importance in both basic and applied research. Because of its many applications in fields as diverse as chemistry, physics, biology, materials science, medicine, and catalysis, applied research on metal nanoparticles (NPs) has been going on for decades. The optical properties and surface Plasmon resonance of metal inorganic nanoparticles are among their unique qualities. Plasmon, also known as the resonance stimulation of a group oscillations within the particle's electron, conduction band, and valence band, is responsible for the brilliant colours seen in noble metal NPs. It is dependent on the size, shape, and composition of the metal NPs as to how strongly they absorb SPR (Kumar *et al.*, 2018). The purpose of this study was to create silver nanoparticles from an extract of the leaves of the *Centella asiatica* plant. FTIR, SEM, TEM, and X-ray diffraction analyses were used to learn more about the synthesised AgNPs. Antimicrobial activity against *Escherichia coli* and *Staphylococcus aureus* was a primary goal in the synthesis of AgNPs.

Materials and Methods

Preparation of Centella asiatica extracts:

Soxhlet extraction was used to get aqueous extracts from the leaves of the *Centella asiatica* plant. The leaves of a *Centella asiatica* plant were ground into a powder and then evenly placed into a thimble. One thousand millilitres of double-distilled water was then added to the mixture. The extraction process will continue until the solvent in the syphon tube of the extractor has lost all of its colour. Once the *Centella asiatica* had been extracted, it was left to chill overnight before being diluted to a volume of one thousand millilitres using double-distilled water.

Preparation of silver nanoparticles using Centella asiatica extracts:

An amount of silver nitrate equivalent to around 1 mM was dissolved in 90 ml of double-distilled water. The *Centella asiatica* plant extracts were combined with the metal solution to create a 100 ml solution. The shift in colour was seen with the

naked eye, and images were taken. After that, the solution was maintained in a magnetic stirrer so that it could be used later in the process of creating nanoparticles. Nanoparticle synthesis was characterised by means of FTIR, SEM, TEM, and XRD.

FTIR Spectrometer:

Organic chemistry, polymer science, petrochemical engineering, the pharmaceutical sector, and food analysis are just some of the many applications for FTIR (Fourier Transform Infrared) spectrometers. The mechanism of chemical reactions and the identification of unstable chemicals may be studied using FTIR spectrometers when combined with chromatography. The infrared range is the vibrational spectrum of molecules. The gap in vibrational energy establishes the absorption peak frequency. Absorption peaks may be counted as evidence of a molecule's degree of vibrational freedom. Absorption peak strength is associated with dipole moment fluctuation and the potential for energy level transitions. Infrared absorption spectroscopy is very helpful since it can be used to study any kind of material, including gases, liquids, and solids. Since most organic molecules and inorganic ions absorb light between 4000 and 400 cm^{-1}, this is the most often utilised area for infrared absorption spectroscopy.

Scanning Electron Microscope (*SEM*):

The size distribution of silver nanoparticles was studied by SEM. SEM was utilised to evaluate the particle size in relation to both bilk and nano particles. The JEOL MODEL JSM 6390 SEM was used to capture the picture.

Transmission, Electron, Microscopy:

Focusing a narrow electron beam onto a subject allows us to observe very small things (often on size of a few nanometers to 100 nm) using the TEM microscope method. It is possible that some of the electrons in an electron beam will be scattered depending on the density of the medium it passed through. The microscopy would provide an image of the substance when the stationary electrons collide with the light source at the microscope's base. Electron microscopy (TEM) with Image J processing software was utilised to identify the Silver nanoparticles' sizes, size distributions, and shapes. Thus, the silver nanoparticles had spherical shapes and typically measured less than 20 nm in size. This effect of laser fluence occurs because these factors affect the cavitation bubble and the plasma generated throughout the procedure. Because of this, the cavitation bubble remains stable for a longer period of time, producing larger particles (Tsuji *et al.*, 2007).

X-Ray Diffraction (*XRD*):

Materials' atomic or molecular structure may be examined by X-ray diffraction (XRD). It is non-destructive and has the best results with crystalline substances. Since the substance being analysed is often reduced to a powder form, x-ray powder diffraction is a common name for the method. Light undergoes diffraction whenever it contacts an opening, a barrier, or the edge of an object. Its severity is determined by the magnitude of the wavelength in comparison to the aperture through which it must pass. Software (such as crystal impact match 2 and diamond 3) may be used to sketch the structure of inorganic materials using XRD as a fingerprint area. Observed data are shown by the blue line. Each colour along the red line represents a different match in the doped sample.

Results and Discussion

Analysis of FTIR:

FTIR is used to identify the functional group of the prepared Nanoparticles (Fig. 1). The sample shows absorption at 449 cm^{-1}, 560 cm^{-1}, 613 cm^{-1}, 898 cm^{-1},1058 cm^{-1},1110 cm^{-1}, 1318 cm^{-1},1378 cm^{-1},1400 cm^{-1}, 1634 cm^{-1}, 1743 cm^{-1}, 2076 cm^{-1}, 2238 cm^{-1},2856 cm^{-1}, 2925 cm^{-1} and 3405 cm^{-1}. Normally adsorption shows in 2800 -3600 cm^{-1} is due to the removal of OH molecule. 449 cm^{-1} was assigned Microcrystals and the peaks are dependent on the axial ratio (c\a) of the crystal.

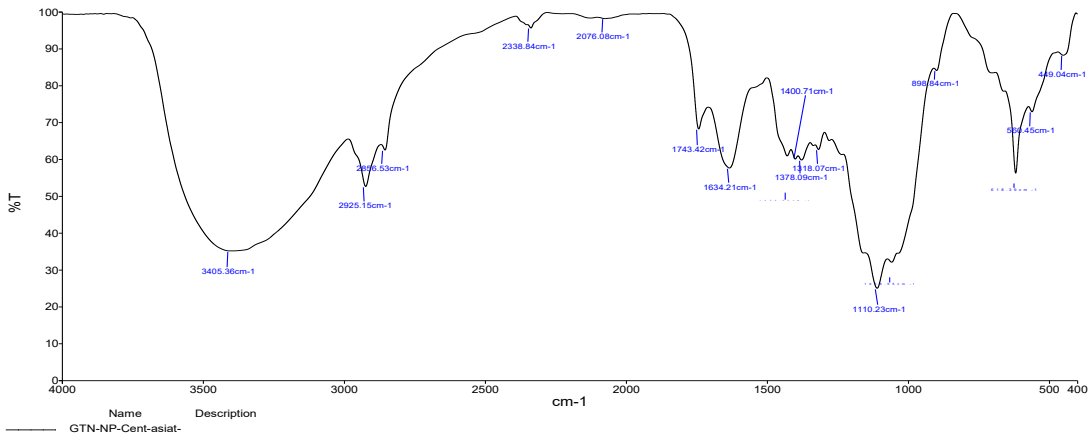

Fig. 1: FTIR of prepared AgO_2.

Table 1: FTIR Spectrum for Sample

Wave Length	Function Group
449 cm^{-1}	Microcrystals and the position the peaks are dependent on the axial ratio (c\a) of the crystal
560 cm^{-1}	Ag-O bonding vibration mode lattice
613 cm^{-1}	carbon metal bond
898 cm^{-1}	=C-H out of plane bonding mode (aromatic ring).
1058 cm^{-1}	C-O strecting mode (Ether).
1110 cm^{-1}	C=O bending mode
1318cm^{-1}, 1378 cm^{-1}, 1400 cm^{-1}	C-O-H bending
1634 cm^{-1}	C=O stretching mode (conjugation of aldehyde with two aromatic rings)

560 cm^{-1} was assigned for Ag-O bonding vibration mode lattice. 613 cm^{-1} was assigned for carbon metal bond. 898 $cm^{-1}$was assigned for =C-H out of plane bonding mode (aromatic ring). 1058 cm^{-1}C-O stretching mode (Ether). 1110 cm^{-1} was assigned for C=O bending mode. 1318 cm^{-1}, 1378 cm^{-1}, 1400 cm^{-1} was assigned for C-O-H bending. 1634 cm^{-1} was assigned for C=O stretching mode (conjugation of aldehyde with two aromatic rings) (Table 1) (Park *et al.*, 2011).

Scanning electron microscopy (*SEM*):

It is utilised to discover the shape and size of the particle. Figure 2 is a scanning electron microscopy (SEM) picture of the sample (AgO_2); based on this image, we may infer that the morphology of the pure particles is spherical, and that the dopped nanoparticles also take on this shape and size. To produce the particles, spheres are used. The particle is not uniformly dispersed. The dimensions are between 20 and 60 nm. Possible environmental causes include high levels of air moisture and other reasons. Particles in the picture have an average size of 20-60 nm (Park *et al.*, 2011).

Transmission Electron Microscope (*TEM*):

Transmission electron microscopy data on Ag-O include particle size, size distribution, shape, degree of agglomeration, etc. Nanoparticles of Ag-Oi powder may be seen in these images. Using a Transmission Electron Microscope, we can validate the typical crystal form and size. Based on the TEM overview pictures shown in Figure 3,

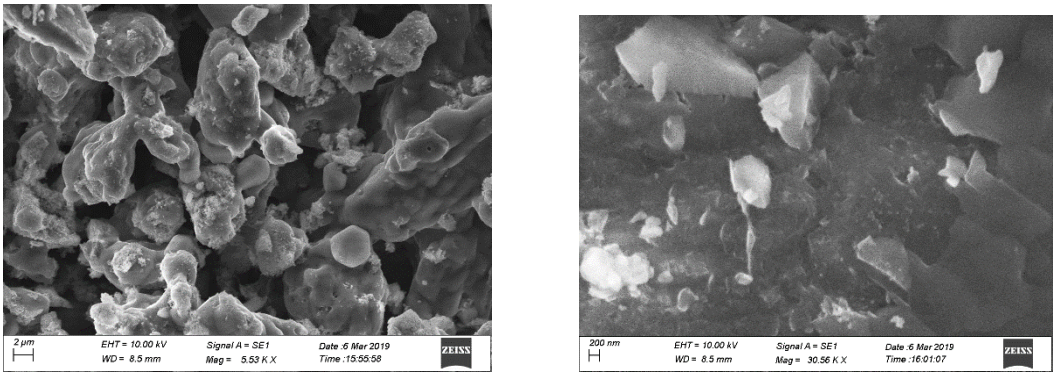

(a) (b)

Fig. 2a, b: SEM Image of AgO_2

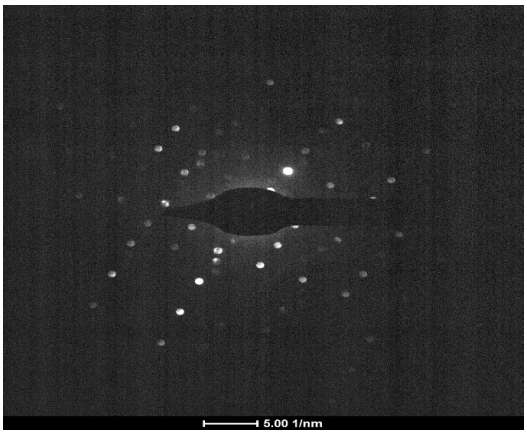

Fig. 3: TEM of prepared AgO_2.

we can infer that the nanoparticles have a regular shape and range in size from 10 to 64 nm. Most of the particles have been shown to take on a spherical form. A portion of a selected area electron diffraction (SAED) pattern is seen in Figure 3. In the SAED pattern, reflections 111, 020, 202, 311, 513, and 060 miller planes describe the spherical structure with the F-43 m space group, indicating that the powder is highly crystalline.

Nanoparticles, as seen in transmission electron microscopy (TEM) pictures, have a spherical shape and no clustering. From what can be seen in the picture, the nanoparticles have a cubical shape.

X-Ray Diffraction (*XRD*):

Software (such as crystal impact match 2 and diamond 3) may be used to sketch the structure of inorganic materials using XRD as a fingerprint area. For each match in the doped sample, the blue line represents the observed data and the red line represents the matched data (Fig. 4). The cubic arrangement of the particles in AgO^2's lattice, the F-43 m spacegroup, and the atomic distance of 4.81600 for the Ag-O band are all evident. The high intensity and d value of 2.7805 in the XRD analysis indicate that the sample is quite pure (96-710-9247 ref data number). Based on atomic distance measurements, it is clear that the procedure makes use of ideal grain sizes and orientations. High-intensity peaks with d-values of 2.7805(111) and 1.7027(111) both have hkl values of 202. According to the SEM report, the grain size of the samples is less than 100 nm, and the two hkl values demonstrate that the samples are 99.9 per cent pure. There is a one-to-one

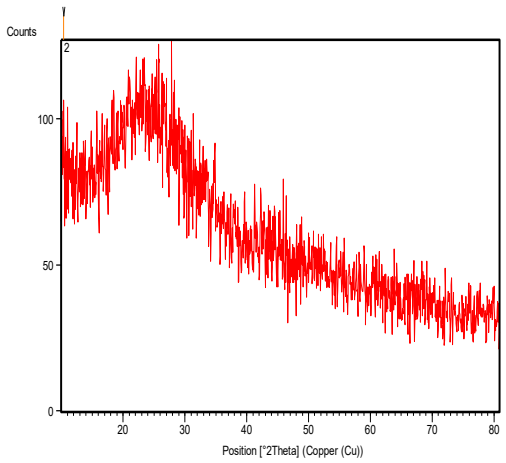

Fig. 4(a): X-Ray of sample AgO_2.

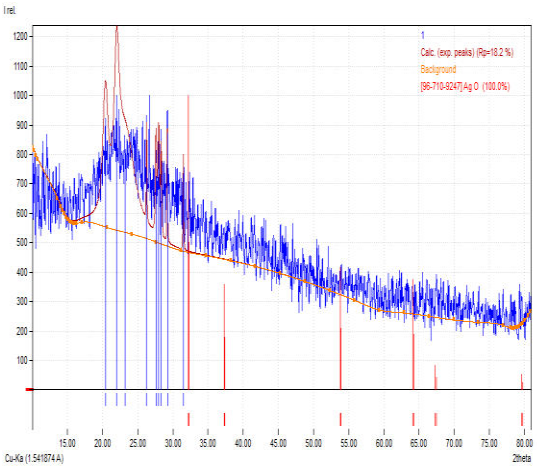

Fig. 4(b): Smoothed Background Data for XRD of AgO_2.

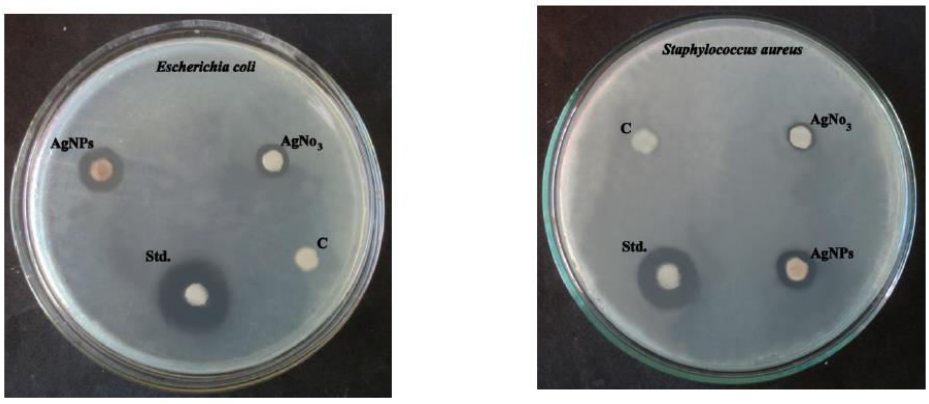

Fig. 5: Antibacterial activity against *E. coli* and *Staphylococcus aureus*

correspondence between the measured unit cell size and the published values (Rynkevic *et al.*, 2017; Rynkevic *et al.*, 2019).

Antibacterial activity against E. coli:

The generation of silver nanoparticles by a wide variety of microorganisms is extensively documented; nevertheless, the potential of marine microbes for this trait has received the least amount of investigation. In the current investigation, a bacterial strain that had been isolated from seawater was used (Fig. 5). Antibacterial activity against therapeutically significant pathogens, such as *Escherichia coli* and *Staphylococcus aureus*, was shown by the biosynthesized AgNPs (Diaconeasa *et al.*, 2015).

Conclusion

We found that *Centella asiatica*'s extract protected steel against rust and corrosion. X-ray diffraction analysis reveals that AgO_2 has a cubic lattice structure with particles that are F-43m in space group atomic distance for Ag-O band is 4.81600. Since the d-value measured by XRD is so low, 2.7805, this indicates that the sample is very pure (96-710-9247 ref data number). Based on atomic distance measurements, it is clear that the procedure makes use of ideal grain sizes and orientations. Both the hkl value of the first, high-intensity peak with a d-value of 2.7805 (111), and the hkl value of the second, high-intensity peak with a d-value of 1.7027, and hkl value of 202

indicate that the samples are 99% pure and perfectly ordered in size. Microscopy reveals that the particle is not evenly dispersed. The dimensions are between 20 and 60 nm. Possible environmental causes include high levels of air moisture and other reasons. The picture shows that particles have an average size of 20-60 nm. The FTIR method is used to determine the kind of functional group present in the synthesised Nanoparticles. SEM analysis has established the size of the AgNPs. Nanoparticles have a spherical form with very minimal aggregation, as shown in transmission electron microscopy pictures. From what can be seen in the picture, the nanoparticles have a cubical shape.

References

Adams WW and Baughman RH. (2005) Retrospective: Richard E. Smalley (1943-2005). Science 310(5756): 1916.

Bhattacharjee A and Ahmaruzzaman M. (2015) Photocatalytic-degradation and reduction of organic compounds using SnO_2 quantum dots (via a green route) under direct sunlight. RSC Adv. 5(81): 66122-66133.

Buzea C, Pacheco II and Robbie K. (2007) Nanomaterials and nanoparticles: sources and toxicity. Biointerphases 2(4): MR17-71.

Chavali MS and Nikolova MP. (2019) Metal oxide nanoparticles and their applications in nanotechnology. SN Appl Sci. 1(6): 1-30.

Diaconeasa Z, Barbu-Tudoran L, Coman C, Leopold L, Mesaros, A, Pop O, Rugina D, Stefan R, Tabaran F, Tripon S and Socaciu C. (2015) Cerium oxide nanoparticles and its cytotoxicity human lung cancer cells. Romanian Biotechnol Letts. 20(4): 10679-10687.

Karkaj OS, Salouti M, Sorouri R and Derakhshan FK. (2012) Biosynthesis of silver nanoparticles by *Bacillus bacteria* Pajoohandeh J. 17(3): 142-147.

Kumar H, Venkatesh N, Bhowmik H and Kuila A. (2018) Metallic nanoparticle: a review. Biomed J Sci Tech Res. 4(2): 3765-3775.

Nath D and Banerjee P. (2013) Green nanotechnology–a new hope for medical biology. Environ Toxicol Pharmacol. 36(3): 997-1014.

Park HG, Oh JH and Lee JS. (2011) Assembly-based titration for the determination of monodisperse plasmonic nanoparticle concentrations using DNA. Analytical Chem. 83(12): 4989-4995.

Rynkevic Rita, Martins P, Fernandes A, Vange J, Monica RG, Radoslaw AW, Tristan M, Anton WB and Deprest J. (2019) In vitro simulation of in vivo degradation and cyclic loading of novel degradable electrospun meshes for prolapse repair. Polymer Testing 78: 105957.

Rynkevic R, Martins P, Pereira F, Ramião N and Fernandes AA. (2017) In vitro study of the mechanical performance of hernia mesh under cyclic loading. J Materials Sci Materials Med. 28(11): 1-7.

Saini R, Saini S and Sharma S. (2010) Nanotechnology: the future medicine. J Cutan Aesthet Surg. 3 (1): 32-33.

Tsuji T, Okazaki Y, Tsuboi Y and Tsuji M. (2007) Nanosecond time-resolved observations of laser ablation of silver in water. Japanese J Appl Phys. 46(4R): 1533.